J|A|C|S
ARTICLES
Published on Web 12/05/2006

Iridium−Iron−Monocarborane Clusters from Oxidative Insertion Reactions of [IrCl(CO)(PPh$_3$)$_2$] with Ferracarborane Anions

Andreas Franken, Thomas D. McGrath,* and F. Gordon A. Stone*

Contribution from the Department of Chemistry & Biochemistry, Baylor University, Waco, Texas 76798-7348

Received July 14, 2006; E-mail: tom_mcgrath@baylor.edu; gordon_stone@baylor.edu

Abstract: The nine-vertex ferracarborane salt [N(PPh$_3$)$_2$][7,7,7-(CO)$_3$-*closo*-7,1-FeCB$_7$H$_8$] (**1**) reacts with an excess of [IrCl(CO)(PPh$_3$)$_2$] in the presence of Tl[PF$_6$] to form, successively, the bimetallic species [7,7,9,9,9-(CO)$_5$-7-PPh$_3$-*closo*-7,9,1-IrFeCB$_6$H$_7$] (**3**), in which one {BH}$^-$ vertex has formally been subrogated by an {Ir(CO)$_2$(PPh$_3$)} unit, and the trimetallic complex [6,7,9-{Ir(CO)(PPh$_3$)$_2$}-7,9-(μ-H)$_2$-7,9,9-(CO)$_3$-7-PPh$_3$-*closo*-7,9,1-IrFeCB$_6$H$_6$] (**5**), which contains an {FeIr$_2$} triangle. The {FeIrCB$_6$} core in **5** resembles that in **3** with, in addition, the Fe···Ir connectivity being spanned by an {Ir(CO)(PPh$_3$)$_2$} fragment and the consequent Fe−Ir and Ir−Ir bonds bridged by hydrido ligands. In contrast to the above, treatment of the 10-vertex diferracarborane salt [N(PPh$_3$)$_2$][6,6,6,10,10,10-(CO)$_6$-*closo*-6,10, 1-Fe$_2$CB$_7$H$_8$] (**2**) with the same reagents yields two very different, trimetallic complexes, namely [8,10-{Ir(μ-PPh$_2$)(Ph)(CO)(PPh$_3$)}-8-(μ-H)-6,6,6,10,10-(CO)$_5$-*closo*-6,10,1-Fe$_2$CB$_7$H$_7$] (**6**) and [6,7,10-{Fe(CO)$_3$}-6-(μ-H)-6,10,10,10-(CO)$_4$-6-PPh$_3$-*closo*-6,10,1-IrFeCB$_7$H$_7$] (**7**). In **6**, an exo-polyhedral {IrPh(CO)(PPh$_3$)} moiety is attached to a {*closo*-6,10,1-Fe$_2$CB$_7$} framework via a PPh$_2$-bridged Fe−Ir bond and a B−H⇀Ir agostic-type linkage, the iridium center formally having inserted into one P−Ph bond of a PPh$_3$ unit. Complex **7** contains an {IrFeCB$_7$} cluster core, with an exo-polyhedral {Fe(CO)$_3$} moiety bridging a {BIrFe} triangular face and with an additional Ir−H−Fe bridge. However, this metal atom arrangement reveals that iridium and iron moieties have exchanged exo- and endo-polyhedral sites with respect to the 10-vertex metallacarborane. X-ray diffraction studies upon **3**, **5**, **6**, and **7** confirmed their novel structural features; some preliminary reactivity studies upon these compounds are also reported.

Introduction

The assembly of "hybrid clusters", that is, species that contain both metal and (hetero)borane cluster units, is an area that has intrigued and challenged cluster chemists for some time and which continues to present significant synthetic obstacles.[1] Such compounds may display structural and electronic properties typical of both boron- and metal-based clusters and also unique features at the interface of the two. However, synthetic routes to these species are often limited as borane derivatives may be rather reducing, resulting in elimination of the metallic portion. Activation of the boron reagent to open and accept multiple metal centers is often also necessary. Conversely, the reducing tendency of boranes has in some cases been useful in encouraging the growth of very high nuclearity clusters.[2]

We have been investigating the possibility of stepwise addition of metal centers to metallacarborane clusters as a possible route to polymetallic cluster hybrids. Such an approach has the additional advantage that it can provide access to heteropolymetallic products by judicious choice of the added metal reagents. Specifically, we have employed metallacarborane complexes containing monocarbon carborane ligands, because the resulting clusters often retain an overall anionic charge as a consequence of the high formal charge (typically 3− or more) upon the carborane fragment itself.[3] Thus, addition of an electrophilic transition metal−ligand fragment to a metallacarborane anion can afford products containing multiple metal centers. Among the latter class, we have recently synthesized bi-, tri-, and tetrametallic derivatives of 11-vertex rhenium−,[1k,4,5] manganese−,[6] and molybdenum−monocarbo-

(1) Examples include: (a) Venable, T. L.; Sinn, E.; Grimes, R. N. *Inorg. Chem.* **1982**, *21*, 904. (b) Wynd, A. J.; Robbins, S. E.; Welch, D. A.; Welch, A. J. *J. Chem. Soc., Chem. Commun.* **1985**, 819. (c) Do, Y.; Knobler, C. B.; Hawthorne, M. F. *J. Am. Chem. Soc.* **1987**, *109*, 1853. (d) Bown, M.; Fontaine, X. L. R.; Greenwood, N. N.; MacKinnon, P.; Kennedy, J. D.; Thornton-Pett, M. *J. Chem. Soc., Dalton Trans.* **1987**, 2781. (e) Carr, N.; Gimeno, M. C.; Stone, F. G. A. *J. Chem. Soc., Dalton Trans.* **1990**, 2247. (f) Jeffery, J. C.; Jelliss, P. A.; Stone, F. G. A. *J. Chem. Soc., Dalton Trans.* **1994**, 25. (g) Nishiara, Y.; Deck, K. J.; Shang, M.; Fehlner, T. P. *Organometallics* **1994**, *13*, 4510. (h) Liao, Y.-H.; Mullica, D. F.; Sappenfield, E. L.; Stone, F. G. A. *Organometallics* **1996**, *15*, 5102. (i) Lei, X.; Shang, M.; Fehlner, T. P. *Organometallics* **2000**, *19*, 5226. (j) Ghosh, S.; Fehlner, T. P.; Noll, B. C. *Chem. Commun.* **2005**, 3080. (k) McGrath, T. D.; Du, S.; Hodson, B. E.; Stone, F. G. A. *Organometallics* **2006**, *25*, 4444.

(2) For example: (a) Schmid, G.; Pfeil, R.; Boese, R.; Brandermann, F.; Meyer, S.; Calis, G. H. M.; van der Velden, J. W. A. *Chem. Ber.* **1981**, *114*, 3634. (b) Schmid, G.; Huster, W. *Z. Naturforsch. B* **1986**, *41*, 1028. See also: (c) Hall, K. P.; Mingos, D. M. P. *Prog. Inorg. Chem.* **1984**, *32*, 237.

(3) (a) McGrath, T. D.; Stone, F. G. A. *J. Organomet. Chem.* **2004**, *689*, 3891. (b) McGrath, T. D.; Stone, F. G. A. *Adv. Organomet. Chem.* **2005**, *53*, 1.

(4) Du, S.; Kautz, J. A.; McGrath, T. D.; Stone, F. G. A. *Organometallics* **2003**, *22*, 2842.

(5) Du, S.; Kautz, J. A.; McGrath, T. D.; Stone, F. G. A. *Angew. Chem., Int. Ed.* **2003**, *42*, 5728.

(6) Du, S.; Jeffery, J. C.; Kautz, J. A.; Lu, X. L.; McGrath, T. D.; Miller, T. A.; Riis-Johannessen, T.; Stone, F. G. A. *Inorg. Chem.* **2005**, *44*, 2815.

Chart 1

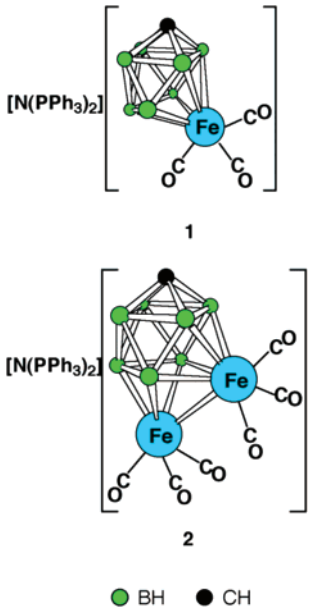

ranes,[7] including a unique pair of tetrametallic "butterfly" complexes that are supported by a metallacarborane substrate. As part of these studies, we are also investigating reactions of the newly available[8] ferracarborane salts $[N(PPh_3)_2][7,7,7\text{-}(CO)_3\text{-}closo\text{-}7,1\text{-}FeCB_7H_8]$ (**1**) and $[N(PPh_3)_2][6,6,6,10,10,10\text{-}(CO)_6\text{-}closo\text{-}6,10,1\text{-}Fe_2CB_7H_8]$ (**2**) (see Chart 1) with cationic transition metal fragments. Whereas reactions of fragments such as $\{Cu(PPh_3)\}^+$ or $\{Ag(PPh_3)\}^+$ with **1** and **2** give relatively simple bi- and trimetallic complexes, respectively,[8] we have found that use of Vaska's compound, $[IrCl(CO)(PPh_3)_2]$, ostensibly a source of the $\{Ir(CO)(PPh_3)_2\}^+$ moiety, affords both discrete and condensed cluster products. These novel and often unexpected species are the subject of this report. (Vertex numbering in the closed 9- and 10-vertex clusters discussed herein is shown in Chart 2.)

Chart 2

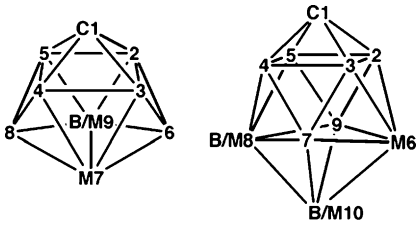

Results and Discussion

Syntheses and Structural Studies. Three neutral iridium−iron−carborane compounds, $[7,7,9,9,9\text{-}(CO)_5\text{-}7\text{-}PPh_3\text{-}closo\text{-}7,9,1\text{-}IrFeCB_6H_7]$ (**3**), $[6,8,8,8\text{-}(CO)_4\text{-}6\text{-}H\text{-}6\text{-}PPh_3\text{-}10\text{-}OPPh_3\text{-}closo\text{-}6,8,1\text{-}IrFeCB_7H_7]$ (**4**), and $[6,7,9\text{-}\{Ir(CO)(PPh_3)_2\}\text{-}7,9\text{-}(\mu\text{-}H)_2\text{-}7,9,9\text{-}(CO)_3\text{-}7\text{-}PPh_3\text{-}closo\text{-}7,9,1\text{-}IrFeCB_6H_6]$ (**5**) (see Chart 3), were prepared by reaction of the ferracarborane salt **1** with an excess of the iridium synthon $[IrCl(CO)(PPh_3)_2]$, with Tl$[PF_6]$ added to remove chloride as insoluble TlCl. Although

Chart 3

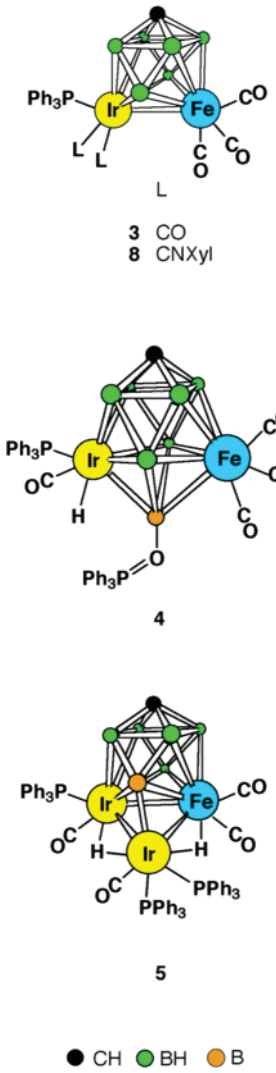

complexes **3** and **5** were obtained in good yields, compound **4** was only a minor product and was often isolated only in very low and variable amounts. The compounds were separable by column chromatography on silica gel and were characterized by the data listed in Tables 1−3. However, the structures of all three products initially were definitively established by X-ray diffraction studies, the results of which are depicted in Figures 1−3, respectively, and are appropriately discussed before the compounds' spectral data.

As is immediately apparent from Figure 1 and Chart 3, compound **3** is a single-cluster metallacarborane. It consists of a nine-vertex polyhedron, with $\{Ir(CO)_2(PPh_3)\}$ and $\{Fe(CO)_3\}$ vertexes in adjacent five-coordinate sites and joined by a metal−metal bond (Ir(1)−Fe(1) = 2.7128(11) Å), and with the carbon atom in a four-coordinate position, all of these sites being consistent with established preferences.[9,10] The metal−metal distance here is similar to that (2.706(2) Å) in the iridaferrabo-

(7) Lei, P.; McGrath, T. D.; Stone, F. G. A. *Chem. Commun.* **2005**, 3706.
(8) Franken, A.; McGrath, T. D.; Stone, F. G. A. *Organometallics* **2005**, *24*, 5157.
(9) (a) Williams, R. E. *Adv. Inorg. Chem. Radiochem.* **1976**, *18*, 67. (b) Ott, J. J.; Gimarc, B. M. *J. Am. Chem. Soc.* **1986**, *108*, 4303.
(10) (a) Grimes, R. N. In *Comprehensive Organometallic Chemistry*; Wilkinson, G., Abel, E. W., Stone, F. G. A., Eds.; Pergamon Press: Oxford, U.K., 1982; Vol. 1, Section 5.5. (b) Grimes, R. N. In *Comprehensive Organometallic Chemistry II*; Abel, E. W., Stone, F. G. A., Wilkinson, G., Eds.; Pergamon Press: Oxford, U.K., 1995; Vol. 1, Chapter 9.

Table 1. Analytical and Physical Data

compd	color	ν_{max}(CO)[a]/cm^{-1}	anal[b] (%) C	anal[b] (%) H
[7,7,9,9,9-(CO)$_5$-7-PPh$_3$-*closo*-7,9,1-IrFeCB$_6$H$_7$] (**3**)	orange	2071 s, 2031 w, 1985 s	39.3 (39.3)	3.2 (3.0)
[6,7,9-{Ir(CO)(PPh$_3$)$_2$}-7,9-(μ-H)$_2$-7,9,9-(CO)$_3$-7-PPh$_3$-*closo*-7,9,1-IrFeCB$_6$H$_6$] (**5**)	green	2017 s, 1996 s, 1961 s, 1913 s	49.8 (49.6)	3.8 (3.8)
[8,10-{Ir(μ-PPh$_2$)(Ph)(CO)(PPh$_3$)}-8-(μ-H)-6,6,6,10,10-(CO)$_5$-*closo*-6,10,1-Fe$_2$CB$_7$H$_7$] (**6**)	orange	2050 s, 2045 s, 1996 s, 1951 w	46.9 (47.2)	3.6 (3.5)
[6,7,10-{Fe(CO)$_3$}-6-(μ-H)-6,10,10,10-(CO)$_4$-6-PPh$_3$-*closo*-6,10,1-IrFeCB$_7$H$_7$] (**7**)	yellow-green	2067 s, 2036 s, 2020 s, 1999 s, 1928 m	36.4 (36.1)	3.0 (2.8)
[9,9,9-(CO)$_3$-7,7-(CNXyl)$_2$-7-PPh$_3$-*closo*-7,9,1-IrFeCB$_6$H$_7$] (**8**)	red	2015 s, 1957 s	51.2 (51.0)	4.1 (4.3)
[8,10-{Ir(μ-PPh$_2$)(Ph)(CNXyl)(PPh$_3$)}-8-(μ-H)-6,6,10,10-(CO)$_4$-6-CNXyl-*closo*-6,10,1-Fe$_2$CB$_7$H$_7$] (**9**)	orange	1998 s, 1970 s, 1935 m	51.7 (52.0)[c]	4.4 (4.2)

[a] Measured in CH_2Cl_2; a broad, medium-intensity band observed at ca. 2500−2550 cm^{-1} in the spectra of all compounds is due to B−H absorptions. In addition, ν_{max}(NC): for **8**, 2150 s, 2124 s cm^{-1}; for **9**, 2142 s, 2123 s cm^{-1}. [b] Calculated values are given in parentheses. In addition, % N: for **8**, 2.8 (3.0); for **9**, 2.0 (2.0). [c] Cocrystallized with 1.0 mol equiv of CH_2Cl_2.

Table 2. ^{1}H and ^{13}C NMR Data[a]

compd	^{1}H/δ[b]	^{13}C/δ[c]
3	7.67−7.25 (m, 15H, Ph), 2.13 (br s, 1H, cage CH)	213.7 (Fe−CO), 176.3 (d, *J*(PC) = 9, Ir−CO), 133.7−128.6 (Ph), 19.1 (br, cage C)
5	7.47−6.98 (m, 45H, Ph), 3.67 (br s, 1H, cage CH), −17.31 (dd, *J*(PH$_{transoid}$) = 65, *J*(PH$_{cisoid}$) = 14, 1H, Ir−H−Ir), −18.85 (dd, *J*(PH$_{cisoid}$) = 18 and 10, 1H, Ir−H−Fe)	226.7 (Fe−CO), 169.3 (d, *J*(PC) = 26, Ir$_{endo}$−CO), 167.8 (dd, *J*(PC) = 27 and 27, Ir$_{exo}$−CO), 133.1−127.9 (Ph), 25.8 (br, cage C)
6	7.45−6.81 (m, 30H, Ph), 6.91 (br s, 1H, cage CH), −9.61 (br, 1H, B−H⇀Ir)	219.2 (d, *J*(PC) = 30, Fe(10)−CO), 210.3 (Fe(6)−CO), 178.1 (dd, *J*(PC$_{transoid}$) = 99, *J*(PC$_{cisoid}$) = 6, Ir−CO), 133.6−127.9 (Ph), 103.3 (br, cage C)
7	8.39 (br s, 1H, cage CH), 7.45 (m, 15H, Ph), −17.22 (d, *J*(PH) = 7, 1H, Fe−H−Ir)	212.0 (Fe−CO), 207.7 (Fe−CO), 178.8 (d, *J*(PC) = 14, Ir−CO), 134.5−128.4 (Ph), 106.0 (br, cage C)
8	7.40−7.03 (m, 21H, Ph and C$_6$H$_3$), 2.39 (s, 6H, Me), 2.32 (s, 6H, Me), 1.87 (br s, 1H, cage CH)	217.4 (CO), 138.5 (d, *J*(PC) = 10, C≡N), 135.2−126.7 (Ph and C$_6$H$_3$), 18.6 (Me), 16.2 (br, cage C)
9	7.45−6.82 (m, 36H, Ph and C$_6$H$_3$), 6.70 (br s, 1H, cage CH), 2.19 (s, 6H, Me), 2.09 (s, 6H, Me), −9.85 (br, 1H, B−H⇀Ir)	222.6 (br, CO), 218.1 (br, CO), 215.1 (CO), 212.8 (CO), 173.3 (Fe−C≡N), 141.2 (d, *J*(PC) = 9, Ir−C≡N), 135.7−121.7 (Ph and C$_6$H$_3$), 101.7 (br, cage C), 18.6 (Me), 18.5 (Me)

[a] Chemical shifts (δ) in ppm, coupling constants (*J*) in hertz, and measurements at ambient temperatures in CD_2Cl_2. [b] Resonances for terminal BH protons occur as broad unresolved signals in the range δ ca. −1 to +3. [c] ^{1}H-decoupled chemical shifts are positive to high frequency of $SiMe_4$.

Table 3. ^{11}B and ^{31}P NMR Data[a]

compd	^{11}B/δ[b]	^{31}P/δ[c]
3	40.4 (2B), −11.2 (2B), −12.8 (2B)	8.6
5	108.4 (B(6)), 46.9, −6.7 (2B), −8.1, −14.1	5.1, 2.7, −20.3 (br)
6	34.2 (B(8)), 13.7 (2B), 11.8, 9.9, −9.5, −13.9	137.1 (μ-PPh$_2$), 19.9 (PPh$_3$)
7	80.6 (B(7)), 45.3, 15.7, 8.2, 4.2, −3.6, −12.6	18.9
8	41.2 (2B), −13.4 (4B)	8.7
9	33.6 (B(8)), 13.9 (2B), 12.2 (2B), −10.4, −13.8	125.5 (μ-PPh$_2$), 25.0 (PPh$_3$)

[a] Chemical shifts (δ) in ppm, coupling constants (*J*) in hertz, and measurements at ambient temperatures in CD_2Cl_2. [b] ^{1}H-decoupled chemical shifts are positive to high frequency of BF_3·Et_2O (external); resonances are of unit integral except where indicated. [c] ^{1}H-decoupled chemical shifts are positive to high frequency of 85% H_3PO_4 (external).

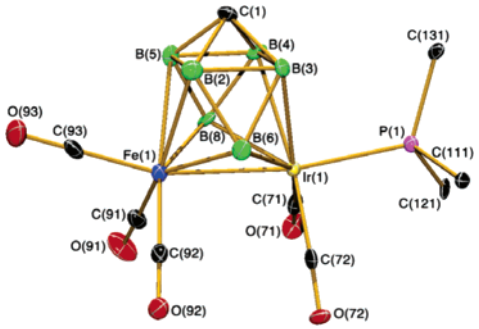

Figure 1. Structure of **3** showing the crystallographic labeling scheme. In this and subsequent figures, thermal ellipsoids are drawn with 40% probability, only chemically significant H atoms are shown, and all but the *ipso* carbon atoms of phosphorus-bound Ph groups are omitted. Selected distances (Å) and angles (deg) are as follows: Ir(1)−Fe(1) 2.7128(11), B(3)−Ir(1) 2.391(8), B(4)−Ir(1) 2.382(8), B(6)−Ir(1) 2.226(8), B(8)−Ir(1) 2.229(7), B(2)−Fe(1) 2.335(8), B(5)−Fe(1) 2.294(8), B(6)−Fe(1) 2.119(9), B(8)−Fe(1) 2.116(7); P(1)−Ir(1)−Fe(1) 162.45(5).

rane [1,1,1,2,2-(CO)$_5$-2,4-(PPh$_3$)$_2$-*closo*-1,2-FeIrB$_5$H$_4$].[11] Clearly, in the reaction, one {BH} vertex of the precursor has been lost, a result that is not uncommon in such reactions,[10,12] and its site formally assumed by the incoming iridium center. The details of the formation of **3** are not entirely clear, but it is notable that the insertion of the iridium fragment is an oxidative process, with the metal oxidation state in the product formally +III compared to +I in the starting Vaska's compound. In this respect, the reaction here may be compared with the earlier reported formation of the nine-vertex iridacarborane [7-CO-7,7-(PPh$_3$)$_2$-*closo*-7,1-IrCB$_7$H$_8$] from [*closo*-1-CB$_7$H$_8$]$^-$ and the same metal reagent, although in that case no Tl[PF$_6$] was added and no {BH} unit was lost.[13] In the present case, the iridium center additionally undergoes PPh$_3$ ⇀ CO substitution, but as

(11) Bould, J.; Rath, N. P.; Fang, H.; Barton, L. *Inorg. Chem.* **1996**, *35*, 2062.
(12) (a) Kennedy, J. D. *Prog. Inorg. Chem.* **1984**, *32*, 519. (b) Kennedy, J. D. *Prog. Inorg. Chem.* **1986**, *34*, 211. (c) Barton, L.; Srivastava, D. K. In *Comprehensive Organometallic Chemistry II*; Abel, E. W., Stone, F. G. A., Wilkinson, G., Eds.; Pergamon Press: Oxford, U.K., 1995; Vol. 1, Chapter 8.
(13) Stíbr, B.; Kennedy, J. D.; Thornton-Pett, M.; Dradáková, E. *Collect. Czech. Chem. Commun.* **1992**, *57*, 1439.

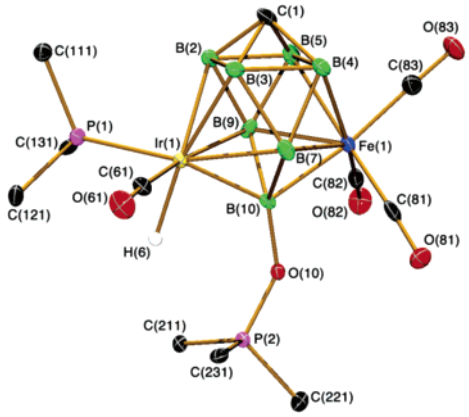

Figure 2. Structure of **4** showing the crystallographic labeling scheme. Selected distances (Å) and angles (deg) are as follows: B(2)−Ir(1) 2.259(6), B(3)−Ir(1) 2.272(6), B(7)−Ir(1) 2.321(6), B(9)−Ir(1) 2.328(6), B(10)−Ir(1) 2.087(6), B(4)−Fe(1) 2.203(6), B(5)−Fe(1) 2.195(7), B(7)−Fe(1) 2.252(6), B(9)−Fe(1) 2.254(6), B(10)−Fe(1) 2.051(5), B(10)−O(10) 1.461(7), O(10)−P(2) 1.546(3), Ir(1)−H(6) 1.689(19); O(10)−B(10)−Fe(1) 112.0(4), O(10)−B(10)−Ir(1) 125.3(3), B(10)−O(10)−P(2) 135.4(3).

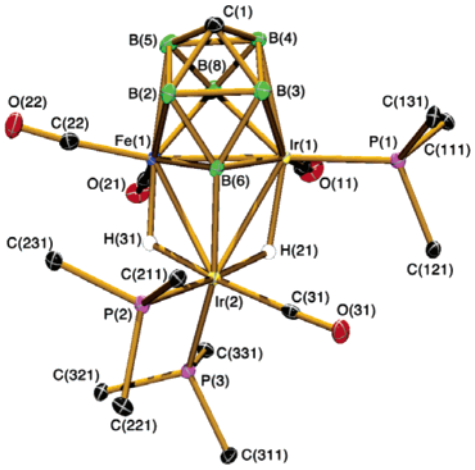

Figure 3. Structure of **5** showing the crystallographic labeling scheme. Selected distances (Å) and angles (deg) are as follows: Ir(1)−Fe(1) 2.6525(5), Ir(1)−Ir(2) 2.9517(3), Ir(1)−H(21) 1.84(3), Ir(1)−B(3) 2.389(3), Ir(1)−B(4) 2.328(4), Ir(1)−B(6) 2.147(3), Ir(1)−B(8) 2.187(4), Fe(1)−B(2) 2.306(4), Fe(1)−B(5) 2.230(4), Fe(1)−B(6) 2.058(3), Fe(1)−B(8) 2.070(4), Fe(1)−H(31) 1.63(3), Fe(1)−Ir(2) 2.8222(5), Ir(2)−B(6) 2.083(4), Ir(2)−H(21) 1.71(3), Ir(2)−H(31) 1.73(3); Fe(1)−Ir(1)−Ir(2) 60.194(12), Ir(1)−Fe(1)−Ir(2) 65.167(12), Fe(1)−Ir(2)−Ir(1) 54.639(10).

the overall reaction forming **3** is clearly complex it would be unwise to speculate further on this one detail of the whole process. An additional feature revealed by the X-ray diffraction study of **3** is elongation of the B(3)···B(4) (2.056(12) Å) and B(2)−B(5) (1.986(12) Å) connectivities compared to typical B−B distances, a feature common in such systems.[8]

The NMR data for compound **3** are consistent with the solid-state structure. Thus, the $^{11}B\{^1H\}$ NMR spectrum reveals a 2:2:2 pattern of resonances, in agreement with molecular C_s symmetry and with loss of one boron vertex of the starting carborane during the reaction. In addition, the ^1H and $^{13}C\{^1H\}$ NMR spectra show resonances at δ 2.13 and 19.1, respectively, typical positions for the cage {CH} unit in a nine-vertex cluster.[8] The latter spectrum also shows two resonances for metal-bound CO ligands, at δ 213.7 and 176.3, that are assigned to the Fe−CO and Ir−CO units, respectively, with the latter showing J(PC) coupling of ca. 9 Hz due to the iridium-bound phosphine. This ligand itself gives rise to a corresponding singlet at δ 8.6 in the $^{31}P\{^1H\}$ NMR spectrum.

The extrusion of a {BH} vertex in the formation of **3** is perhaps surprising given the known[14] stability of 10-vertex systems. However, the identity of compound **4**, whose structure is shown in Figure 2, may provide some suggestions as to the processes involved. The molecule of **4** is again a single-cluster species and consists of a *closo*-10-vertex {6,8,1-IrFeCB$_7$} cluster to which is appended at B(10) a two-electron donor Ph$_3$P═O ligand (B(10)−O(10) = 1.461(7) Å). The latter substituent lowers the overall charge upon the formal {*arachno*-CB$_7$H$_7$-(OPPh$_3$)} carborane moiety to 4− (cf. 5− for the unsubstituted {*arachno*-CB$_6$H$_7$} unit in **3**), and correspondingly the iridium center bears an H$^-$ ligand, rather than a CO group as in **3**, with the overall complex again being neutral. Traces of adventitious O_2 or H_2O in the reaction mixture might have generated Ph$_3$PO molecules from the PPh$_3$ liberated during formation of **3**, or the oxide might be a contaminant in the [IrCl(CO)(PPh$_3$)$_2$] reagent. In our experience, ligand−borane adducts [L·BH$_3$] are often observed (^{11}B NMR) as side products in reactions where boron vertexes may be eliminated. In the present system, arguably, loss of the ligand-substituted B(10) vertex in compound **4** (as [Ph$_3$PO·BH$_3$]) could lead directly to a closed {IrFeCB$_6$} intermediate and thence to compound **3** itself by CO scavenging.

Spectroscopic data for compound **4** (see the Experimental Section) are fully consistent with the solid-state structure. In particular, the $^{11}B\{^1H\}$ NMR spectrum shows four signals in the ratio 1:2:2:2, with the highest frequency signal (δ 94.6) remaining a singlet upon retention of proton coupling. This is assigned to the unique vertex bearing the O═PPh$_3$ substituent: the high chemical shift is typical of a four-connected boron atom in such clusters[13,15] and the attached oxygen donor would be expected also to cause further deshielding. Correspondingly, the phosphine oxide group gives rise to a singlet (δ 46.2) in the $^{31}P\{^1H\}$ NMR spectrum, with the iridium-bound PPh$_3$ found to higher field (δ 12.0) and similar to that in compound **3**. Notably, there is also tentative evidence of a 10-PPh$_3$ analogue of compound **4** in $^{11}B\{^1H\}$ NMR spectra of the reaction mixture, with a low-field doublet (δ 76.1, J(PB) = 120 Hz) that again has the high chemical shift typical of a four-connected boron in 10-vertex metallacarborane clusters. Such a complex could also be an intermediate that leads (via Ph$_3$P·BH$_3$ loss) to compound **3** in a manner similar to that described above for **4**. Attempts to isolate this proposed B-PPh$_3$ species, however, were unsuccessful, perhaps suggestive that it is indeed transitory en route to compound **3**.

The structure of compound **5** was rather more unexpected than that of either **3** or **4**. It is seen (Figure 3) to consist of the same nine-vertex {*closo*-7,9,1-IrFeCB$_6$} core as in **3**, but with an additional iridium moiety appended exo-polyhedrally. Indeed, we have been able to confirm experimentally that reaction of bimetallic **3** with an excess of [IrCl(CO)(PPh$_3$)$_2$]/Tl[PF$_6$] does afford the trimetallic product **5**. In the latter, the intracluster Fe−Ir distance Ir(1)−Fe(1) is 2.6525(5) Å, significantly shorter than that in **3**, while the B(3)···B(4) (2.038(5) Å) and B(2)−

(14) Schleyer, P. v. R.; Najafian, K. *Inorg. Chem.* **1998**, *37*, 3454.
(15) See also, for example: (a) Evans, W. E.; Dunks, G. B.; Hawthorne, M. F. *J. Am. Chem. Soc.* **1973**, *95*, 4565. (b) Briguglio, J. J.; Sneddon, L. G. *Organometallics* **1986**, *5*, 327.

B(5) (1.991(5) Å) separations are similarly elongated as those in **3**. The exo-polyhedral iridium center in **5** is an {Ir(CO)-$(PPh_3)_2$} fragment that has displaced one CO group from each of the cluster metal vertexes and which is attached via two metal−metal bonds to form an $\{FeIr_2\}$ triangle, with distances Ir(1)−Ir(2) = 2.9517(3) and Fe(1)−Ir(2) = 2.8222(5) Å. Both of the latter two connectivities are bridged by hydrido ligands, which were located in the X-ray diffraction experiment (Ir(1)−H(21) = 1.84(3), Ir(2)−H(21) = 1.71(3), Ir(2)−H(31) = 1.73(3), Fe(1)−H(31) = 1.63(3) Å). The coordination sphere around Ir(2) is completed by a direct Ir−B σ bond (Ir(2)−B(6) = 2.083(4) Å). This last feature is shorter than the η-bonded Ir(1)−B distances in **5** (range 2.147(3)−2.389(3) Å) but similar in length to *exo*-Ir^{III}−B σ bonds in related species (range 2.071(14)−2.163(7) Å).[16]

A further notable aspect of the structure of **5** is that B(6) is also bonded to the other two metal atoms (Ir(1)−B(6) = 2.147(3), Fe(1)−B(6) = 2.058(3) Å). Thus, the tetrahedral $\{BIr_2$-Fe} moiety that includes B(6) may be viewed as being fused to the parent $\{IrFeCB_6\}$ cluster via the {B(6)Fe(1)Ir(1)} face, so that overall this species has a condensed "double cluster" architecture. This "capped" *closo*-9-vertex structure in principle would formally be converted to a conventional *closo*-10-vertex one by a diamond−square−diamond operation[17] upon the B(8)Ir(1)Ir(2)Fe(1) "diamond". In cluster electron counting terms,[9a,18] the fused-cage architecture of **5** has *10* skeletal electron pairs (SEPs), as is to be expected for a capped *closo*-9-vertex species. By way of comparison, the cluster skeletons of the precursor **1** (a *closo*-9-vertex species) and of compounds **3** and **4** (*closo*-9- and -10-vertex species, respectively), possess 10, 10, and 11 SEPs, respectively, and thus also conform to the accepted electron counting rules.

All NMR data for compound **5** are in accord with the results of the X-ray study. In its $^{11}B\{^1H\}$ NMR spectrum, four separate resonances with relative intensities 1:1:2:1:1 are seen, of which one very deshielded signal (δ 108.4) remains a singlet in the fully coupled ^{11}B spectrum and may be assigned to the boron atom involved in the direct B(6)−Ir linkage.[19] The ^1H NMR spectrum shows diagnostic multiplet resonances for the two metal-bridging hydrides, at δ −17.31 (dd, $J(PH_{transoid})$ = 65 Hz and $J(PH_{cisoid})$ = 14 Hz) and −18.85 (dd, $J(PH_{cisoid})$ = 18 and 10 Hz); no mutual coupling between the two hydrides could be resolved, and both signals become singlets in a $^1H\{^{31}P\}$ NMR spectrum. Of these data, the former resonance is assigned to the Ir−H−Ir bridge on the basis of the large coupling expected for a *transoid* arrangement, so that the resonance showing the smaller coupling must be due to the Ir−H−Fe bridge. A broad peak at δ 3.67 in the same spectrum, corresponding in intensity to one proton, may be assigned to the cage CH group, with the corresponding carbon resonance at δ 25.8 in the $^{13}C\{^1H\}$ NMR spectrum. Therein are also seen three CO resonances: at δ 226.7 for the Fe−CO groups, and at δ 169.3 (d, J(PC) = 26 Hz) and 167.8 (dd, J(PC) = 27 and 27 Hz) for the carbonyls on the endo- and exo-polyhedral iridium centers, respectively. As would be expected, the $^{31}P\{^1H\}$ NMR spectrum shows three singlet resonances, but with no mutual J(PP) coupling discernible. The first resonance (δ 5.1) becomes a broad doublet-of-doublets in a ^1H-coupled ^{31}P NMR spectrum (J(HP) ca. 65 and 10 Hz) and is assigned to P(2) of the PPh_3 group on Ir(2) (crystallographic numbering), which is *transoid* with respect to the Ir−H−Ir hydride. The second ^{31}P signal (δ 2.7) shows a small doublet splitting (J(HP) ca. 10 Hz) upon retention of proton coupling and is attributed to the phosphine bound to Ir(1). No J(HP) coupling could be discerned for the third peak (δ −20.3), as it is broadened by unresolved $^{11}B-^{31}P$ coupling and hence is assigned to P(3) of the PPh_3 group that is *transoid* to the Ir−B σ bond.

Chart 4

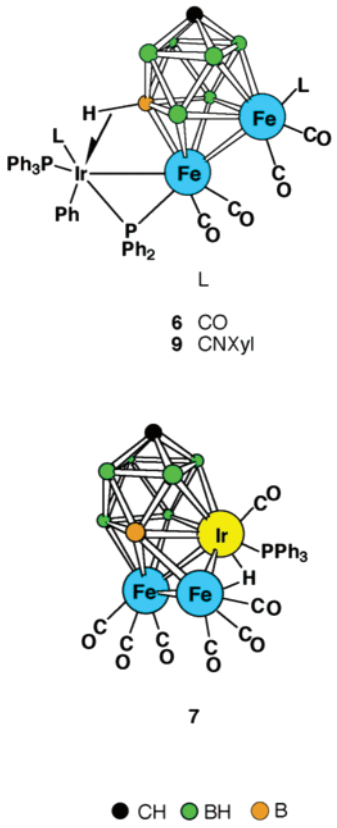

7

In contrast to the formation of **3**−**5** from the monoiron precursor **1**, the compounds [8,10-{Ir(μ-PPh_2)(Ph)(CO)(PPh_3)}-8-(μ-H)-6,6,6,10,10-$(CO)_5$-*closo*-6,10,1-$Fe_2CB_7H_7$] (**6**) and [6,7,-10-{$Fe(CO)_3$}-6-(μ-H)-6,10,10,10-$(CO)_4$-6-PPh_3-*closo*-6,10,1-$IrFeCB_7H_7$] (**7**) (Chart 4) are formed when the diiron compound **2** was stirred with $[IrCl(CO)(PPh_3)_2]$ and $Tl[PF_6]$ in CH_2Cl_2 at ambient temperature. These two compounds can conveniently be separated by column chromatography on silica and were characterized by the data in Tables 1−3. As before, their precise constitutions were determined by single-crystal X-ray diffraction studies. These experiments revealed the structures shown in Figures 4 and 5, respectively.

Compound **6** (Figure 4) is seen to be a single-cluster species and retains the {*closo*-Fe_2CB_7} core of the precursor **2**, with the appendage of an iridium unit in an exo-polyhedral site. Thus, compound **6**, like the anion of **2**, is a *closo*-10-vertex cluster

(16) (a) Churchill, M. R.; Hackbarth, J. J. *Inorg. Chem.* **1975**, *14*, 2047. (b) Fernandez, J. R.; Helm, G. F.; Howard, J. A. K.; Pilotti, M. U.; Stone, F. G. A. *J. Chem. Soc., Dalton Trans.* **1990**, 1747. (c) Bae, J.-Y.; Lee, Y.-J.; Kim, S.-J.; Ko, J.; Cho, S.; Kang, S. O. *Organometallics* **2000**, *19*, 1514. (d) Herberhold, M.; Yan, H.; Milius, W.; Wrackmeyer, B. *J. Organomet. Chem.* **2000**, *604*, 170. (e) Herberhold, M.; Yan, H.; Milius, W.; Wrackmeyer, B. *J. Chem. Soc., Dalton Trans.* **2001**, 1782. (f) Herberhold, M.; Yan, H.; Milius, W.; Wrackmeyer, B. *Chem.−Eur. J.* **2002**, *8*, 388.
(17) Lipscomb, W. N. *Science* **1966**, *153*, 373.
(18) (a) Wade, K. *Adv. Inorg. Chem. Radiochem.* **1976**, *18*, 1. (b) Mingos, D. M. P. *Acc. Chem. Res.* **1984**, *17*, 311.
(19) Brew, S. A.; Stone, F. G. A. *Adv. Organomet. Chem.* **1993**, *35*, 135.

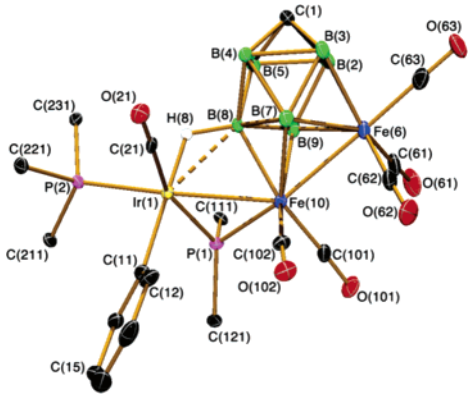

Figure 4. Structure of **6** showing the crystallographic labeling scheme. Selected distances (Å) and angles (deg) are as follows: Fe(6)−Fe(10) 2.5626(9), B(2)−Fe(6) 2.182(6), B(3)−Fe(6) 2.178(5), B(7)−Fe(6) 2.203(5), B(9)−Fe(6) 2.212(5), Ir(1)−Fe(10) 2.7321(6), Fe(10)−P(1) 2.2379(12), B(7)−Fe(10) 2.185(5), B(8)−Fe(10) 2.025(5), B(9)−Fe(10) 2.224(5), Ir(1)−C(11) 2.122(4), Ir(1)−P(1) 2.2982(11), Ir(1)···B(8) 2.348(4), Ir(1)−H(8) 1.65(4); P(1)−Fe(10)−Fe(6) 146.76(4), Fe(6)−Fe(10)−Ir(1) 136.28(3), Fe(10)−P(1)−Ir(1) 74.06(3).

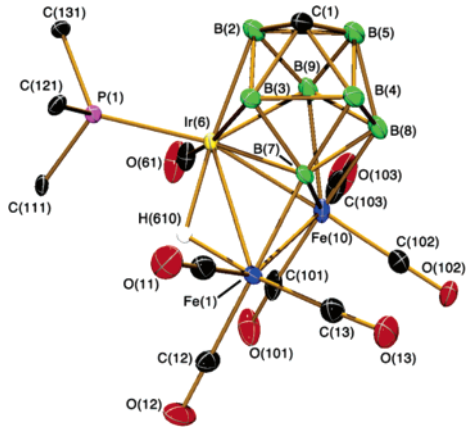

Figure 5. Structure of **7** showing the crystallographic labeling scheme. Selected distances (Å) and angles (deg) are as follows: Ir(6)−Fe(1) 2.7806(6), Ir(6)−Fe(10) 2.6036(7), Ir(6)−H(610) 1.79(4), B(2)−Ir(6) 2.225(5), B(3)−Ir(6) 2.246(5), B(7)−Ir(6) 2.216(5), B(9)−Ir(6) 2.247(5), B(7)−Fe(10) 2.074(5), B(8)−Fe(10) 2.140(5), B(9)−Fe(10) 2.269(5), Fe(1)−Fe(10) 2.6486(9), Fe(1)−H(610) 1.68(5), Fe(1)−B(7) 2.004(4); Fe(10)−Ir(6)−Fe(1) 58.825(19), Ir(6)−Fe(10)−Fe(1) 63.92(2), Fe(10)−Fe(1)−Ir(6) 57.25(2).

with the anticipated skeletal electron count of 11 SEPs. An alternative view of **6** is as a fused-cage species: a *closo*-10-vertex cluster edge-fused to a triangle; this arrangement (i.e., including the triangle) possesses 12 SEPs but this is also consistent with accepted electron counting rules.

The exo-iridium fragment in **6** is attached via a B−H ⇀ Ir agostic-type interaction, with Ir(1)···B(8) = 2.348(4) Å and Ir(1)−H(8) = 1.65(4) Å, and by an Fe−Ir bond (Ir(1)−Fe(10) = 2.7321(6) Å) that involves the iron vertex that is in the four-connected cluster site. This latter connectivity is bridged by a PPh_2 moiety (Fe(10)−P(1) = 2.2379(12), Ir(1)−P(1) = 2.2982(11) Å). The origin of the phosphide is clearly a PPh_3 ligand of the precursor iridium reagent, as the iridium center bears a σ-bonded Ph group (Ir(1)−C(11) = 2.122(4) Å). Thus, the iridium center may be considered formally to have oxidatively inserted into a P−Ph bond of one phosphine, rather than into the ferracarborane as in the formation of **3**−**5**. Such cleavage reactions for PPh_3 and other ligands bonded to transition metal centers have been known for several decades[20] and are well-documented as being of considerable importance in some catalytic processes.[21] The present reaction system, forming **6**, also has a close parallel in the reactions of the related iridium reagent $[IrMe(CO)(PR_3)_2]$ with $[MH(CO)_3(\eta\text{-}C_5H_5)]$ (M = Mo, W; R = *p*-tolyl,[22] Ph[23]). In these, the reactions are proposed to occur between an $\{Ir(CO)(PR_3)_2\}^+$ cation and an $\{M(CO)_3(\eta\text{-}C_5H_5)\}^-$ anion, of which the latter may be thought of as quasi-isolobal[24] with the $[Fe(CO)_3\{\eta\text{-cage}\}]^-$ anion of compound **2**.

The NMR data for compound **6** (Tables 2 and 3) are in complete agreement with the structure established by the X-ray diffraction study. In the $^{11}B\{^1H\}$ NMR spectrum, six signals are seen, in the ratio 1:2:1:1:1:1, showing an absence of molecular symmetry (the integral-2 peak being a 1 + 1 coincidence), consistent with the solid-state structure. The peak to highest frequency (δ 34.2) shows only a very small broadening (*J*(HB) not resolved) upon retention of proton coupling and is assigned to the B−H ⇀ Ir group.[19] In the ^1H NMR spectrum, the same unit gives rise to a broad resonance at δ −9.61. There is a further signal in this spectrum at δ 6.91 that is in the region characteristic for a cage CH unit in such 10-vertex cages,[8] with a corresponding and also characteristic broad resonance at δ 103.3 in the $^{13}C\{^1H\}$ NMR spectrum. Three signals for CO ligands are also seen therein, with those bound to Fe(6) appearing as one singlet (δ 210.3) and the signal for those bound to Fe(10) showing doublet structure (δ 219.2; *J*(PC) = 30 Hz) due to coupling with the phosphorus of the μ-PPh_2 unit. The third CO resonance, for the Ir-bound ligand, is a doublet-of-doublets at δ 178.1 and shows a large coupling (*J*(PC) = 99 Hz) due to the *transoid* phosphide, with an additional smaller coupling (*J*(PC) = 6 Hz) to the *cisoid* PPh_3 ligand. As expected, the $^{31}P\{^1H\}$ NMR spectrum shows two resonances, at δ 137.1 and 19.9, which may be assigned on the basis of their chemical shifts to the μ-PPh_2 and Ir−PPh_3 groups, respectively, with no mutual coupling discernible between the two types of phosphorus nuclei.

The structure determined for compound **7** is shown in Figure 5. The data were of sufficient quality that the site of the metal−metal bridging hydride that is evident in NMR data (see below) could reasonably be confirmed and, crucially, the heavy atom arrangement was definitively established. Specifically, complex **7** contains a central {*closo*-6,10,1-$IrFeCB_7$} cluster and an exo-polyhedral iron unit, so that an iridium fragment has replaced the formerly five-connected iron vertex at the 6-position in the precursor and this $\{Fe(CO)_3\}$ moiety now caps a {BIrFe} triangular face. Like compound **5**, the overall structure of **7** may be viewed as a condensed double cluster: here the 10-vertex {*closo*-6,10,1-$IrFeCB_7$} iridaferracarborane is face-fused with a capping $\{IrFe_2B\}$ tetrahedron (Fe(1)−Ir(6) = 2.7806(6), Fe(1)−Fe(10) = 2.6486(9), Ir(6)−Fe(10) 2.6036(7), B(7)−Ir(6) = 2.216(5), B(7)−Fe(10) = 2.074(5), B(7)−Fe(1) = 2.004(4) Å). The exo-polyhedral Fe(1)−B(7) connectivity is a

(20) For example: Bradford, C. W.; Nyholm, R. S. *J. Chem. Soc., Chem. Commun.* **1972**, 87.
(21) Leading reviews include: (a) Garrou, P. E. *Chem. Rev.* **1985**, *85*, 171. (b) van Leeuwen, P. W. N. M. *Appl. Catal., A* **2001**, *212*, 61. (c) Parkins, A. W. *Coord. Chem. Rev.* **2006**, *250*, 449.
(22) McFarland, J. M.; Churchill, M. R.; See, R. F.; Lake, C. H.; Attwood, J. D. *Organometallics* **1991**, *10*, 3530.
(23) Dahlenburg, L.; Halsch, E.; Wolski, A.; Moll, M. *J. Organomet. Chem.* **1993**, *463*, 227.
(24) Hoffmann, R. *Angew. Chem., Int. Ed. Engl.* **1982**, *21*, 711.

direct σ bond, and a bridging hydride is located along the Ir(6)−Fe(1) edge (Ir(6)−H(610) = 1.79(4), Fe(1)−H(610) = 1.68(5) Å). This hydride, located crystallographically, may be viewed as having migrated from a terminal site upon B(7) to the metal−metal bridging position, with the exo-{Fe(CO)$_3$} moiety perhaps being involved via formation of a B(7)−H(7) ⇀ Fe(1) agostic-type interaction. Such hydride migration has been observed previously where, for example, polymetallic compounds containing B−H ⇀ Ru moieties have transformed to species containing a direct B−Ru σ bond and an Ru-(μ-H)-Ru bridging hydride.[1h,25]

Spectroscopic data characterizing compound **7** are given in Tables 1−3. The ^{1}H NMR spectrum was informative, displaying a diagnostic doublet resonance (J(PH) = 7 Hz) at δ −17.22. This is in the region typical of metal−metal bridging hydrides, and the observation of coupling to the iridium-bound phosphine confirms that this hydride is located on an Ir−Fe edge. Its site upon the Ir(6)−Fe(1), rather than Ir(6)−Fe(10), connectivity is intuitively more reasonable given the coordination environments at each metal atom and is supported by the X-ray diffraction results discussed above. A further ^{1}H NMR signal, at δ 8.39 and also of relative intensity one, is in the region characteristic for a cage CH in 10-vertex *closo*-metalla-monocarborane cages.[8] In the ^{11}B{^{1}H} NMR spectrum, there are seven separate resonances, consistent with the absence of molecular symmetry, of which one (δ 80.6) remains a singlet in the fully proton-coupled spectrum and hence may be assigned to B(7), which is directly σ-bonded to iron.[19] Three signals for CO ligands are evident in the ^{13}C{^{1}H} NMR spectrum of **7**, of which the two for the two {Fe(CO)$_3$} groups are singlets (δ 212.0 and 207.7), while the Ir−CO resonance (δ 178.8) is a doublet (J(PC) = 14 Hz), as expected.

The observation that the iridium center in **7** now occupies a cluster vertex, apparently having exchanged sites with one of the iron vertexes, is highly unusual in metallacarborane chemistry. However, we have recently observed similar behavior where the addition of cationic {M(CO)$_2$}$^+$ fragments (M = Rh, Ir) to 11-vertex rhenium− and manganese−monocarborane dianions resulted in ejection of {M′(CO)$_3$} vertexes (M′ = Re, Mn) and the {M(CO)$_2$} unit assuming the endo-polyhedral cluster site.[26] In the present case, parallels can certainly be drawn, as both the {M′(CO)$_3$} and {Fe(CO)$_3$} fragments are conical, d^6 groups. However, in the 11-vertex system a 12-vertex intermediate for the process was proposed, with both metal centers part of a closed {MM′CB$_9$} cluster prior to extrusion of the {M′(CO)$_3$} moieties; supporting evidence for this came from a closely related platinum−manganacarborane system.[6] In the case of compound **7**, an analogous mechanism would require expansion of the 10-vertex {Fe$_2$CB$_7$} core of the precursor **2** to an 11-vertex {IrFe$_2$CB$_7$} species, a suggestion that would be at odds with the known stability of 10-vertex systems.[14] Moreover, although the face-capped, *closo*-10-vertex configuration of **7** has 11 SEPs and so conforms to conventional electron counting rules, the {IrFe$_2$CB$_7$} intermediate proposed above would be a nonconventional 11-SEP, *closo*-11-vertex species that might not be expected to be stable and hence its reversion to a capped 10-vertex geometry.

These comments notwithstanding, it may also be of relevance to note that we have recently observed formation of a 13-vertex cupradicarborane from addition of {Cu(PPh$_3$)}$^+$ to a 13-vertex rhenadicarborane, a process that arguably might also involve a vertex-expanded bimetallic intermediate.[27] Indeed, it is becoming increasingly clear that established patterns of cluster stability may not hold so rigidly when multiple metal centers are present. Clearly, further work is required in this and related systems to understand fully the processes involved and to isolate and identify perhaps other side products and intermediates.

Preliminary Reactivity Studies. We have performed some preliminary investigations upon the reactivity of compounds **3**, **5**, **6**, and **7**. In particular, we have attempted to substitute metal-bound CO groups by other donor ligands and also have examined some possible reactions of the Ir−Ph unit and the stability of the bridging phosphide moiety in **6**. Most of these reactions were unsuccessful. Perhaps not surprisingly, compounds **5** and **7** appear rather unstable upon reaction with donor ligands, and to date we have been unable to isolate any identifiable products from treatment of these complexes with isocyanides or phosphines in the presence of Me$_3$NO. Likewise, both **3** and **6** undergo considerable decomposition upon treatment with a range of donor groups. However, both **3** and **6** do readily give substitution products upon reaction with CNXyl (Xyl = C$_6$H$_3$Me$_2$-2,6) in the presence of Me$_3$NO, affording the products [9,9,9-(CO)$_3$-7,7-(CNXyl)$_2$-7-PPh$_3$-*closo*-7,9,1-IrFeCB$_6$H$_7$] (**8**) and [8,10-{Ir(μ-PPh$_2$)(Ph)(CNXyl)(PPh$_3$)}-8-(μ-H)-6,6,10,10-(CO)$_4$-6-CNXyl-*closo*-6,10,1-Fe$_2$CB$_7$H$_7$] (**9**), respectively (Charts 3 and 4).

X-ray diffraction studies were necessary initially to establish with certainty which CO groups had been replaced. These experiments were straightforward; their results have been included as Supporting Information, and the structures are summarized in Charts 3 and 4. From these it is seen that, in compound **8**, both of the iridium-bound CO groups in the precursor **3** have been replaced by CNXyl ligands, while in compound **9**, the sole Ir−CO in **6** has been converted to Ir−CNXyl and one of the carbonyls bound to five-connected Fe(6) has also been substituted by CNXyl. Other structural features of **3** and **6** are retained upon formation of **8** and **9**, and the skeletal electron counts are unchanged upon CO substitution.

Data characterizing compounds **8** and **9** are given in Tables 1−3, and they are fully in accord with the X-ray diffraction results. The presence of two equivalent CNXyl ligands in **8** gives rise to a single set of resonances in typical positions and with the expected intensities in the ^{1}H and ^{13}C{^{1}H} NMR spectra, while the same spectra for **9** reveal as anticipated two sets of signals for the two different isocyanide ligands. These spectra also indicate little change in the chemical shifts of the atoms in the cage {CH} units of both **8** and **9** compared to their precursors, while the ^{1}H NMR resonance (δ −9.85) for the B−H ⇀ Ir linkage in **9** is slightly shielded compared with that for **6**. Likewise, the ^{11}B{^{1}H} and ^{31}P{^{1}H} NMR spectra for **8** and **9** are similar to those of the precursors **3** and **6** and confirm no major structural or electronic changes upon substitution of CO groups by CNXyl.

(25) (a) Ellis, D. D.; Franken, A.; Stone, F. G. A. *Organometallics* **1999**, *18*, 2362. (b) McGrath, T. D.; Stone, F. G. A.; Sukcharoenphon, K. *Dalton Trans.* **2005**, 2500.

(26) McGrath, T. D.; Du, S.; Hodson, B. E.; Lu, X. L.; Stone, F. G. A. *Organometallics* **2006**, *25*, 4452.

(27) Hodson, B. E.; McGrath, T. D.; Stone, F. G. A. *Organometallics* **2005**, *24*, 3386.

Conclusion

Reactions of the ferracarborane anions of compounds **1** and **2** with a source of the cationic $\{Ir(CO)(PPh_3)_2\}^+$ fragment, derived from Vaska's compound, result in a variety of product types that arise from different oxidative insertion processes involving the iridium moiety. With **1**, the iridium center oxidatively inserts into the ferracarborane cluster, ultimately giving **3** following elimination of a {BH} vertex: the nature of the side product **4**, obtained in very low yield, implies a possible mechanism for the boron vertex loss. Further iridium reagent apparently inserts into a B−H bond of the iridaferracarborane **3** itself, with the final trimetallic, fused cluster product **5** exhibiting several novel structural features. In contrast, reaction of **2** with the iridium reagent can follow two different oxidative insertion paths: A formal insertion into a P−Ph bond affords **6**, of which the starting diferracarborane cluster is essentially unchanged; whereas formation of **7** appears to require insertion of the iridium moiety into the metallacarborane, transiently giving a proposed 11-vertex trimetallacarborane intermediate that extrudes an iron center into an exo-polyhedral site. Both of the complexes **5** and **7** can be considered to be fused, "double cluster" species of a class that is highly unusual in metallcarborane chemistry.

Experimental Section

Syntheses. All reactions were carried out under an atmosphere of dry, oxygen-free nitrogen using Schlenk line techniques. Solvents were stored over and distilled from appropriate drying agents under nitrogen prior to use. Petroleum ether refers to that fraction of boiling point 40−60 °C. Chromatography columns (typically ca. 18 cm in length and ca. 2 cm in diameter) were packed with silica gel (Acros, 60−200 mesh). Filtration through Celite typically employed a plug ca. 5 cm in length and ca. 2 cm in diameter. Elemental analyses were performed by Atlantic Microlab, Inc., Norcross, GA, upon crystalline or microcrystalline samples that had been dried overnight in vacuo. Where residual solvent remained after drying, its presence and approximate proportion were confirmed by integrated ^{1}H NMR spectroscopy, and this was factored into the calculated microanalysis data. NMR spectra were recorded at the following frequencies (MHz): ^{1}H, 360.1; ^{13}C, 90.6; ^{11}B, 115.5; ^{31}P, 145.8. The compounds **1**,[8] **2**,[8] and [IrCl(CO)(PPh$_3$)$_2$][28] were prepared according to the literature; all other materials were used as received. Note that quoted yields for compounds **3**−**7** are the highest obtained and that these yields are very sensitive to reaction time and conditions.

Synthesis of [7,7,9,9,9-(CO)$_5$-7-PPh$_3$-*closo*-7,9,1-IrFeCB$_6$H$_7$], [6,8,8,8-(CO)$_4$-6-H-6-PPh$_3$-10-OPPh$_3$-*closo*-6,8,1-IrFeCB$_7$H$_7$], and [6,7,9-{Ir(CO)(PPh$_3$)$_2$}-7,9-(μ-H)$_2$-7,9,9-(CO)$_3$-7-PPh$_3$-*closo*-7,9,1-IrFeCB$_6$H$_6$]. The compounds **1** (0.19 g, 0.25 mmol), [IrCl(CO)(PPh$_3$)$_2$] (0.40 g, 0.5 mmol), and Tl[PF$_6$] (0.18 g, 0.5 mmol) were stirred in CH_2Cl_2 (20 mL) for 48 h. The solvent was removed in vacuo, the residue was extracted with CH_2Cl_2 (2 mL), and the extract was filtered (Celite) and transferred to the top of a chromatography column. Elution with CH_2Cl_2/petroleum ether (1:1) gave an orange fraction from which removal of solvent in vacuo yielded orange microcrystals of [7,7,9,9,9-(CO)$_5$-7-PPh$_3$-*closo*-7,9,1-IrFeCB$_6$H$_7$] (**3**; 0.081 g; 44%). Further elution, using CH_2Cl_2/petroleum ether (3:2), gave a small, yellow fraction from which removal of solvent in vacuo afforded yellow microcrystals of [6,8,8,8-(CO)$_4$-6-H-6-PPh$_3$-10-OPPh$_3$-*closo*-6,8,1-IrFeCB$_7$H$_7$] (**4**; 0.013 g; 5%). Finally, a green fraction was eluted with CH_2Cl_2/petroleum ether (4:1) from which removal of solvent in vacuo yielded green microcrystals of [6,7,9-{Ir(CO)(PPh$_3$)$_2$}-7,9-(μ-H)$_2$-7,9,9-(CO)$_3$-7-PPh$_3$-*closo*-7,9,1-IrFeCB$_6$H$_6$] (**5**; 0.09 g; 12%). Data for compound **4**: IR (CH_2Cl_2): ν_{max}(CO) = 2028 s, 1997 s, 1960 s cm^{-1}. NMR (CD_2Cl_2, 298 K): δ_H 8.00−6.98 (m, 30H, Ph), 3.31 (br s, 1H, cage CH), −9.62 (d, J(PH) = 30, 1H, Ir−H); δ_B 94.6 (1B, B(10)), 2.9 (2B), −11.3 (2B), −17.4 (2B); δ_P 46.2 (s, OPPh$_3$), 12.0 (br s, IrPPh$_3$).

Synthesis of [8,10-{Ir(μ-PPh$_2$)(Ph)(CO)(PPh$_3$)}-8-(μ-H)-6,6,6,10,-10-(CO)$_5$-*closo*-6,10,1-Fe$_2$CB$_7$H$_7$] and [6,7,10-{Fe(CO)$_3$}-6-(μ-H)-6,-10,10,10-(CO)$_4$-6-PPh$_3$-*closo*-6,10,1-IrFeCB$_7$H$_7$]. Compound **2** (0.23 g, 0.25 mmol), [IrCl(CO)(PPh$_3$)$_2$] (0.20 g, 0.25 mmol), and Tl[PF$_6$] (0.090 g, 0.25 mmol) were stirred in CH_2Cl_2 (20 mL) for 18 h. The solvent was removed in vacuo, the residue was extracted with CH_2Cl_2 (2 mL), and the extract was filtered (Celite) and applied to a chromatography column. Elution with CH_2Cl_2/petroleum ether (2:3) gave successively a yellow-green fraction and an orange fraction that yielded green microcrystals of [6,7,10-{Fe(CO)$_3$}-6-(μ-H)-6,10,10,10-(CO)$_4$-6-PPh$_3$-*closo*-6,10,1-IrFeCB$_7$H$_7$] (**7**; 0.077 g; 37%) and orange microcrystals of [8,10-{Ir(μ-PPh$_2$)(Ph)(CO)(PPh$_3$)}-8-(μ-H)-6,6,6,10,-10-(CO)$_5$-*closo*-6,10,1-Fe$_2$CB$_7$H$_7$] (**6**; 0.140 g; 52%), respectively, after removal of solvent in vacuo.

Reactions with CNXyl. (i) Compound **3** (0.092 g, 0.125 mmol) was dissolved in CH_2Cl_2 (10 mL), CNXyl (0.033 g, 0.25 mmol) and Me_3NO (0.019 g, 0.25 mmol) were added, and the mixture was stirred for 1 h. The solvent was removed in vacuo, and the residue was dissolved in CH_2Cl_2 (1 mL) and transferred to the top of a chromatography column. Elution with CH_2Cl_2/petroleum ether (1:1) gave a red fraction from which removal of solvent in vacuo yielded red microcrystals of [9,9,9-(CO)$_3$-7,7-(CNXyl)$_2$-7-PPh$_3$-*closo*-7,9,1-IrFeCB$_6$H$_7$] (**8**; 0.084 g; 72%).

(ii) Compound **6** (0.140 g, 0.125 mmol) and CNXyl (0.033 g, 0.25 mmol) were dissolved in CH_2Cl_2 (10 mL), and Me_3NO (19 mg, 0.25 mmol) was added. After being stirred for 18 h, the mixture was treated as above to give orange microcrystals of [8,10-{Ir(μ-PPh$_2$)(Ph)(CNXyl)(PPh$_3$)}-8-(μ-H)-6,6,10,10-(CO)$_4$-6-CNXyl-*closo*-6,10,1-Fe$_2$CB$_7$H$_7$] (**9**; 0.130 g; 79%).

X-ray Diffraction Experiments. Experimental data for compounds **3**−**7** are given in the Supporting Information. X-ray intensity data were collected at 110(2) K on a Bruker-Nonius X8 APEX CCD area detector diffractometer using Mo Kα X-radiation (λ = 0.71073 Å). Several sets of narrow data "frames" were collected at different values of θ, for various initial values of ϕ and ω, using 0.5° increments of ϕ or ω. The data frames were integrated using SAINT;[29] the substantial redundancy in data allowed an empirical absorption correction (SADABS[29]) to be applied, based on multiple measurements of equivalent reflections.

All structures were solved using conventional direct methods[29,30] and refined by full-matrix least squares on all F^2 data using SHELXTL version 6.12,[30] with anisotropic thermal parameters assigned to all non-hydrogen atoms. The locations of the cage carbon atoms were verified by examination of the appropriate internuclear distances and the magnitudes of their isotropic thermal displacement parameters. All hydrogen atoms in organic groups, as well as cluster BH and CH hydrogens for **3**, **4**, and **7**, were set riding in calculated positions; other cage BH and CH hydrogens, and metal-bound hydrogens, were allowed positional refinement. All hydrogens had fixed isotropic thermal parameters defined as U_{iso}(H) = 1.2 × U_{iso}(parent), or U_{iso}(H) = 1.5 × U_{iso}(parent) for methyl groups, apart from the metal-bound hydrides whose thermal parameters were refined.

Each molecule of compound **4** cocrystallized with one-half of a molecule of CH_2Cl_2 as solvate in the asymmetric fraction of the unit cell; some restraining of the C−Cl distance (1.76(2) Å; DFIX card in SHELXL[30]) was necessary. In addition, each molecule of compound **6** cocrystallized with one molecule of C_5H_{12} solvate, of which a β-CH_2

(28) Vrieze, K.; Collman, J. P.; Sears, C. T.; Kubota, M. *Inorg. Synth.* **1968**, *11*, 101.

(29) *APEX 2*, version 1.0; Bruker AXS: Madison, WI, 2003−2004.
(30) *SHELXTL*, version 6.12; Bruker AXS: Madison, WI, 2001.

unit was disordered over two sites that were assigned refining complementary occupancies, in the ratio 56:44 at convergence; the C−C distances in this solvate were restrained toward sensible distances (1.54(3) Å; DFIX card in SHELXL[30]).

Acknowledgment. We thank the Robert A. Welch Foundation for support (Grant AA-0006). The Bruker-Nonius X8 APEX diffractometer was purchased with funds received from the National Science Foundation Major Instrumentation Program (Grant CHE-0321214).

Supporting Information Available: Full details of the crystal structure analyses in CIF format, including data for compounds **8** and **9**. This material is available free of charge via the Internet at http://pubs.acs.org.

JA065042N